Creating Patterned Carbon Nanotube Catalysts through the Microcontact Printing of Block Copolymer Micellar Thin Films

Ryan D. Bennett,[†] Anastasios J. Hart,[#] Andrew C. Miller,[†] Paula T. Hammond,[†] Darrell J. Irvine,[‡] and Robert E. Cohen*,[†]

Department of Chemical Engineering, Department of Mechanical Engineering, and Department of Materials Science and Engineering and the Biological Engineering Division, Massachusetts Institute of Technology, 77 Massachusetts Avenue, Cambridge, Massachusetts 02139

Received April 18, 2006. In Final Form: July 14, 2006

We report a route for synthesizing patterned carbon nanotube (CNT) catalysts through the microcontact printing of iron-loaded poly(styrene-*block*-acrylic acid) (PS-*b*-PAA) micellar solutions onto silicon wafers coated with thin aluminum oxide (Al_2O_3) layers. The amphiphilic block copolymer, PS-*b*-PAA, forms spherical micelles in toluene that can form quasi-hexagonal arrays of spherical PAA domains within a PS matrix when deposited onto a substrate. In this report, we dip a poly(dimethylsiloxane) (PDMS) molded stamp into an iron-loaded micellar solution to create a thin film on the PDMS features. The PDMS stamp is then put in contact with a substrate, and uniaxial compressive stress is applied to transfer the micellar thin film from the PDMS stamp onto the substrate in a defined pattern. The polymer is then removed by oxygen plasma etching to leave a patterned iron oxide nanocluster array on the substrate. Using these catalysts, we achieve patterned vertical growth of multiwalled CNTs, where the CNTs maintain the fidelity of the patterned catalyst, forming high-aspect-ratio standing structures.

Introduction

Reliable and facile patterning of substrates is an important technological challenge. Patterning using soft lithography,[1−4] which relies on an elastomeric polymer to replicate a hard master, has successfully emerged as a fast, inexpensive, and straightforward route for patterning substrates.[5] Microcontact printing (μCP) is a soft lithographic patterning technique that has received much attention since its development roughly a decade ago.[6−8] While μCP was originally utilized to pattern self-assembled monolayers of alkane thiols on gold,[7] this technique is also effective in patterning polymeric thin films.[5,9−13]

Amphiphilic block copolymer micelles in organic solvents represent a novel type of polymer solution from which micelles are capable of self-assembling into nanoscale ordered structures when deposited onto a surface.[14−16] These block copolymer micellar systems have been utilized for various applications, including creating inorganic nanoclusters for carbon nanotube (CNT)[15,17] and zinc oxide nanowire growth,[18] protein binding,[19] and magnetic applications.[20] Recently Yun et al.[21] developed a soft-lithographic method for patterning polystyrene-*block*-poly(4-vinylpyridine) (PS-*b*-PVP) micelles onto a substrate utilizing μCP. In this approach, a toluene-based solution of PS-*b*-PVP micelles loaded with $FeCl_3$ was spin-coated onto a poly(dimethylsiloxane) (PDMS) stamp and then transferred to a silicon (Si) substrate through μCP. This route achieved micron-scale patterning of PS-*b*-PVP micellar thin films, which were subsequently oxygen plasma etched to create a monolayer of iron oxide nanoclusters.

In this report, we utilize a μCP approach[22] to pattern poly(styrene-*block*-acrylic acid) (PS-*b*-PAA) micellar thin films as organized catalyst templates for CNT growth. In previous work, CNT growth catalysts have primarily been patterned using lithographic methods following the physical deposition of metal thin films,[23] although some work has been done using block copolymers containing covalently bound iron molecules to create catalysts.[24,25] Using a μCP approach, we pattern a PS-*b*-PAA micellar thin film using a block copolymer micellar inking solution

* To whom correspondence should be addressed. E-mail: recohen@mit.edu.

[†] Department of Chemical Engineering.

[#] Department of Mechanical Engineering.

[‡] Department of Materials Science and Engineering and the Biological Engineering Division.

(1) Whitesides, G. M.; Ostuni, E.; Takayama, S.; Jiang, X. Y.; Ingber, D. E. *Annu. Rev. Biomed. Eng.* **2001**, *3*, 335−373.

(2) Xia, Y. N.; Whitesides, G. M. *Annu. Rev. Mater. Sci.* **1998**, *28*, 153−184.

(3) Kane, R. S.; Takayama, S.; Ostuni, E.; Ingber, D. E.; Whitesides, G. M. *Biomaterials* **1999**, *20*, 2363−2376.

(4) Zhao, X. M.; Xia, Y. N.; Whitesides, G. M. *J. Mater. Chem.* **1997**, *7*, 1069−1074.

(5) Jiang, X. P.; Zheng, H. P.; Gourdin, S.; Hammond, P. T. *Langmuir* **2002**, *18*, 2607−2615.

(6) Kumar, A.; Whitesides, G. M. *App. Phys. Lett.* **1993**, *63*, 2002−2004.

(7) Kumar, A.; Biebuyck, H. A.; Whitesides, G. M. *Langmuir* **1994**, *10*, 1498−1511.

(8) Kumar, A.; Whitesides, G. M. *Science* **1994**, *263*, 60−62.

(9) Wang, M. T.; Braun, H. G.; Kratzmuller, T.; Meyer, E. *Adv. Mater.* **2001**, *13*, 1312−1317.

(10) Yan, L.; Huck, W. T. S.; Zhao, X. M.; Whitesides, G. M. *Langmuir* **1999**, *15*, 1208−1214.

(11) Granlund, T.; Nyberg, T.; Roman, L. S.; Svensson, M.; Inganas, O. *Adv. Mater.* **2000**, *12*, 269−273.

(12) Berg, M. C.; Choi, J.; Hammond, P. T.; Rubner, M. F. *Langmuir* **2003**, *19*, 2231−2237.

(13) Tokuhisa, H.; Hammond, P. T. *Langmuir* **2004**, *20*, 1436−1441.

(14) Bennett, R. D.; Miller, A. C.; Kohen, N. T.; Hammond, P. T.; Irvine, D. J.; Cohen, R. E. *Macromolecules* **2005**, *38*, 10728−10735.

(15) Bennett, R. D.; Xiong, G. Y.; Ren, Z. F.; Cohen, R. E. *Chem. Mater.* **2004**, *16*, 5589−5595.

(16) Boontongkong, Y.; Cohen, R. E. *Macromolecules* **2002**, *35*, 3647−3652.

(17) Fu, Q.; Huang, S. M.; Liu, J. *J. Phys. Chem. B* **2004**, *108*, 6124−6129.

(18) Haupt, M.; Ladenburger, A.; Sauer, R.; Thonke, K.; Glass, R.; Roos, W.; Spatz, J. P.; Rauscher, H.; Riethmuller, S.; Moller, M. *J. Appl. Phys.* **2003**, *93*, 6252−6257.

(19) Spatz, J. P.; Mossmer, S.; Hartmann, C.; Moller, M.; Herzog, T.; Krieger, M.; Boyen, H. G.; Ziemann, P.; Kabius, B. *Langmuir* **2000**, *16*, 407−415.

(20) Yun, S. H.; Sohn, B. H.; Jung, J. C.; Zin, W. C.; Lee, J. K.; Song, O. *Langmuir* **2005**, *21*, 6548−6552.

(21) Yun, S. H.; Sohn, B. H.; Jung, J. C.; Zin, W. C.; Ree, M.; Park, J. W. *Nanotechnology* **2006**, *17*, 450−454.

(22) Kind, H.; Bonard, J.-M.; Emmenegger, C.; Nilsson, L.-O.; Hernadi, K.; Maillard-Schaller, E.; Schlapbach, L.; Forro, L.; Kern, K. *Adv. Mater.* **1999**, *11*, 1285−1289.

(23) (a) Hata, K.; Futaba, D. N.; Mizuno, K.; Namai, T.; Yumura, M.; Iijima, S. *Science*, **2004**, *306*, 1362−1364. (b) Zhang, G. Y.; Mann, D.; Zhang, L.; Javey, A.; Li, Y. M.; Yenilmez, E.; Wang, Q.; McVittie, J. P.; Nishi, Y.; Gibbons, J.; Dai, H. J. *Proc. Natl. Acad. Sci. U.S.A.* **2005**, *102*, 16141−16145.

(24) Lastella, S.; Jung, Y. J.; Yang, H. C.; Vajtai, R.; Ajayan, P. M.; Ryu, C. Y.; Rider, D. A.; Manners, I. *J. Mater. Chem.* **2004**, *14*, 1791−1794.

10.1021/la061054a CCC: $33.50
Published on Web 08/23/2006

that had been previously loaded with $FeCl_3$ onto a Si wafer coated with aluminum oxide (Al_2O_3). Oxygen plasma etching removes the organic components of the micellar thin film leaving a patterned iron oxide nanocluster array. We then utilize the catalytic function of these patterned iron oxide nanocluster arrays, along with our previous knowledge of growth conditions for these catalyst systems,[26] to synthesize patterned arrays of vertically grown multiwalled CNTs (MWCNTs) that are characterized using scanning electron microscopy (SEM). We observe that the fidelity of the pattern is maintained as the CNTs grow vertically from the substrate to heights that are 2 orders of magnitude larger than the characteristic pattern width.

Experimental Section

Materials. PS-*b*-PAA [M_n (PS) = 16 400 g/mol, M_n (PAA) = 4500 g/mol, PDI = 1.05] was used as received from Polymer Source, Inc. PDMS stamps were synthesized by pouring a two-component curable siloxane (Sylgard 184, Dow Corning) over a silicon master with the desired pattern. Anhydrous iron(III) chloride ($FeCl_3$) and toluene (HPLC grade, 99.8%), both obtained from Sigma-Aldrich Co., were used as received. CNTs were synthesized on clean silicon wafers (p-type, Silicon Quest International), which were coated with a 15 nm film of Al_2O_3 by electron beam evaporation using a Temescal VES-2550, with an FDC-8000 Film Deposition Controller. CNT growth[26] was performed in a conventional single-zone atmospheric pressure quartz tube furnace having an inside diameter of 22 mm and a heating zone of 30 cm. Argon (Ar, 99.999%, Airgas), ethylene (C_2H_4, 99.5%, Airgas), and hydrogen (H_2, 99.999%, BOC) were used as received.

Sample Preparation. PS-*b*-PAA was mixed with toluene at a concentration of 5.5 mg/mL and heated to 145 °C for 20 min in a sealed vial to create a spherical block copolymer micellar solution, as presented previously.[14−16] $FeCl_3$ was then added to the micellar solution at a ratio of 5.4 metal ion equiv per carboxylic acid group.[14] Two stamp geometries were utilized: the channeled PDMS stamps had a constant feature height of 400 nm (variable aspect ratio from 2.5 to 20), while the cylindrical post PDMS stamps had a constant aspect ratio of 1. The untreated PDMS stamps were inked by dipping the stamps into the micellar solution with the patterned surface oriented vertically. Maintaining this orientation, the PDMS stamps were submerged in the solution for 3 s, and then removed at a rate of 0.1−2 mm s^{-1}. The PDMS stamps were then allowed to dry for 4 min with the patterned surface oriented vertically, and then rotated to dry for 1 min with the patterned surface oriented horizontally. The PDMS stamps were then placed in contact with an untreated Si substrate or an Al_2O_3-coated Si substrate (previously shown to be an effective supporting layer for CNT growth using Fe-based catalysts[26−28]) for 3−5 min, and a uniaxial compressive stress was applied (approximately 40 kPa). Excessive stamping stress caused the entire stamp (both the raised and recessed features) to contact the substrate (which was easily observed visually during stamping), in which case the applied stress was reduced for proper stamping. The stamps were slowly peeled from the substrate to leave a patterned block copolymer micellar film on the substrate.

The patterned substrates were then oxygen plasma etched (rf plasma, 8−12 MHz) for 15−20 min to remove the polymer thin film, leaving only iron oxide nanoclusters remaining on the substrate.[15] Details about our procedure for synthesizing vertically grown CNTs have been published previously.[26] In brief, the substrate was placed in a quartz tube reactor, covered by a silicon wafer shield, and ramped to 750 °C under a 400 sccm flow of Ar for 30 min. The substrate was held at 750 °C under Ar for 14 min; then

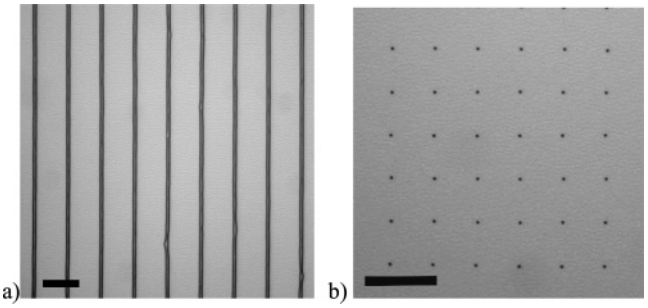

Figure 1. Optical microscope images of PS-*b*-PAA micellar thin films patterned using μCP with a PDMS stamp with a: (a) feature width of 4.5 μm and a periodicity of 9 μm, (b) feature diameter of 4 μm and a periodicity of 6 μm. Scale bar = 10 μm.

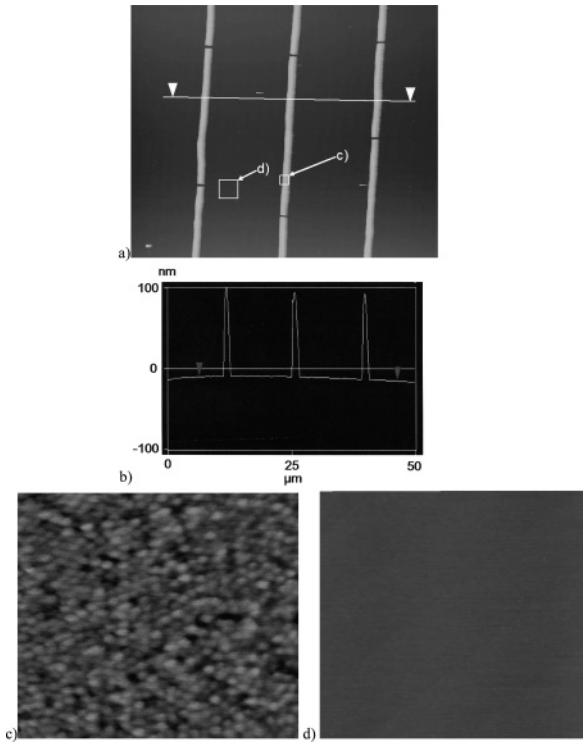

Figure 2. AFM characterization of a PS-*b*-PAA micellar thin film patterned using a PDMS stamp having a channel width of 7 μm and a periodicity of 14 μm. (a) AFM height image (50 × 50 μm scan) showing a patterned PS-*b*-PAA micellar thin film on a Si substrate; (b) plot of individual scan line along the line connecting the two white triangles in panel a; (c) AFM phase image (0.6 × 0.6 μm scan, 50° scale) from the square denoted as "c" in panel a; (d) AFM phase image (2.5 × 2.5 μm scan, 50° scale) from the square area denoted "d" in panel a.

Ar was reduced to 200 sccm, and 500 sccm of H_2 was introduced for 1 min. Ar was then reduced to 0 sccm, and 200 sccm of C_2H_4 was introduced with 500 sccm of H_2 for 15 min. Following growth, the furnace was flushed with Ar and cooled to room temperature.

Characterization. The patterned films were examined using a Leica optical microscope equipped with a Nikon digital camera (DXM 1200F) using Nikon imaging software (ACT-1, Version 2). Images were obtained in reflectance mode. Atomic force microscopy (AFM) images were obtained using a Digital Instruments Dimension 3000 Nanoscope IIIA scanning probe microscope operating in tapping mode using a silicon cantilever. SEM images were obtained using a JEOL 6320FV field-emission high-resolution microscope operating at 5 kV.

Results and Discussion

The optical microscope images in Figure 1 demonstrate the effectiveness of using μCP to pattern PS-*b*-PAA micellar thin

(25) Lu, J. Q.; Kopley, T. E.; Moll, N.; Roitman, D.; Chamberlin, D.; Fu, Q.; Liu, J.; Russell, T. P.; Rider, D. A.; Manners, I.; Winnik, M. A. *Chem. Mater.* **2005**, *17*, 2227−2231.
(26) Bennett, R. D.; Hart, A. J.; Cohen, R. E. *Adv. Mater.*, in press.
(27) de los Arcos, T.; Garnier, M. G.; Seo, J. W.; Oelhafen, P.; Thommen, V.; Mathys, D. *J. Phys. Chem. B* **2004**, *108*, 7728−7734.
(28) Hart, A. J.; Slocum, A. H.; Royer, L. *Carbon* **2006**, *44*, 348−359.

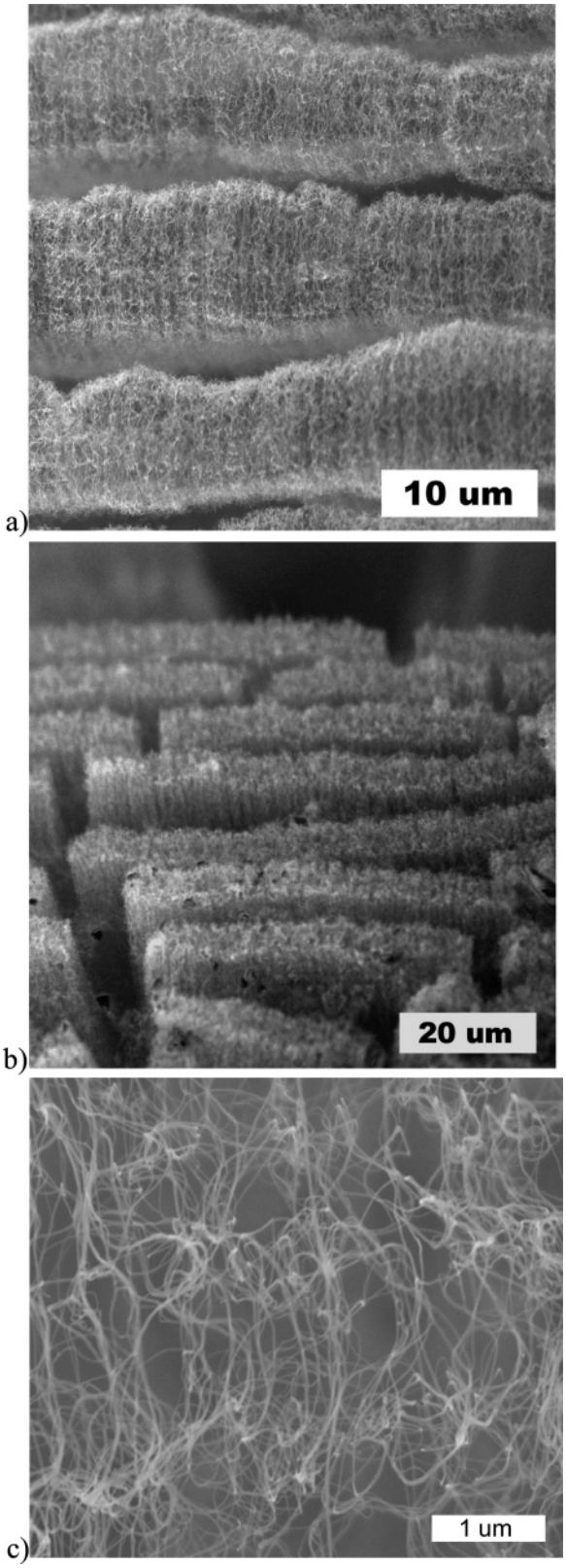

Figure 3. SEM micrographs of vertically grown MWCNT structures grown from an $FeCl_3$-loaded PS-*b*-PAA micellar thin film patterned onto an Al_2O_3-coated Si substrate using a μCP approach with a channeled PDMS stamp with a width of 5 μm and a periodicity of 10 μm. The CNT synthesis used 200/500 sccm of C_2H_4/H_2 at 750 °C for 15 min. (a) Overhead view (0° tilt); (b) side view (70° tilt); (c) higher magnification image of side of vertically grown MWCNT structures (45° tilt).

films in various geometries. The patterns were homogeneous over nearly the entire stamping region (approximately 10 mm^2).

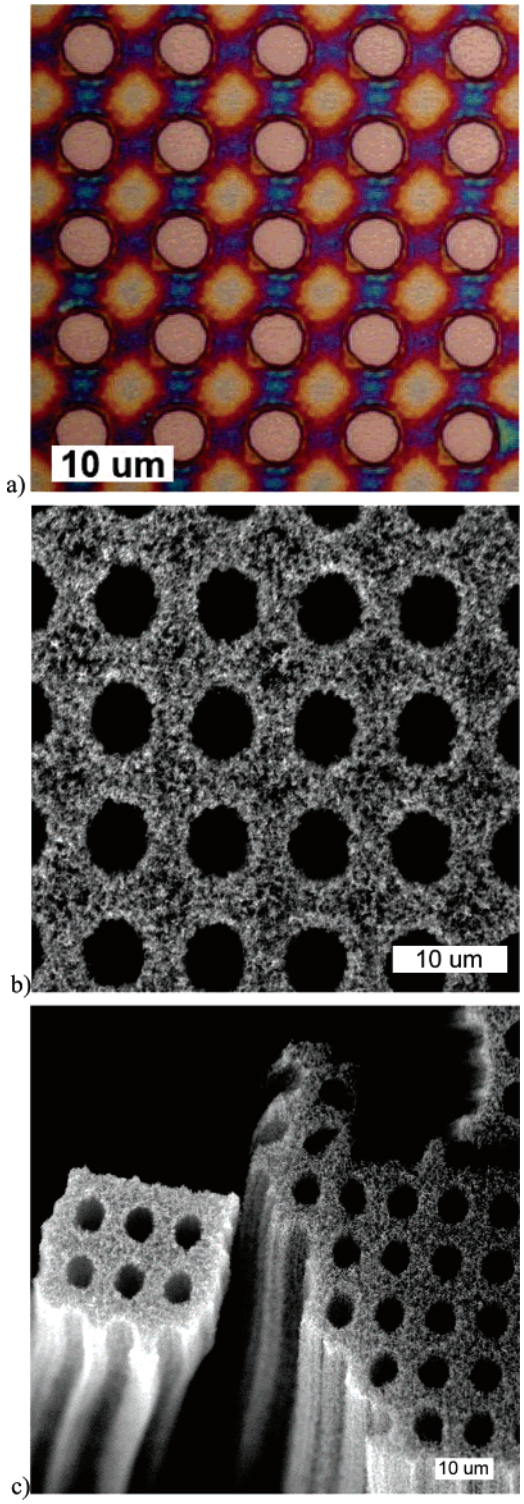

Figure 4. (a) Optical microscope image of an $FeCl_3$-loaded PS-*b*-PAA micellar thin film patterned on an Al_2O_3-coated Si substrate using μCP with an applied pressure of 600 kPa using a PDMS stamp of cylindrical posts with diameters of 4 μm and a periodicity of 8 μm and a removal velocity of 0.2 mm s^{-1}. The lighter areas correspond to bare substrate, while the darker areas correspond to PS-*b*-PAA micellar thin film. (b,c) SEM micrographs of vertically oriented MWCNT structures grown from the substrate shown in panel a after oxygen plasma etching. The CNT synthesis consisted of 200/500 sccm of C_2H_4/H_2 at 750 °C for 15 min. (b) Overhead view (0° tilt); (c) side view (45° tilt).

In both images, the patterned PS-*b*-PAA micellar films had a characteristic width that was considerably smaller than the characteristic width of the PDMS stamp from which they were

printed. In Figure 1a, a PDMS feature width of 4.5 μm led to a PS-*b*-PAA micellar film width of 0.9 μm, while, in Figure 1b, a PDMS feature diameter of 4 μm led to a PS-*b*-PAA micellar film diameter of 0.6 μm. We believe that this effect was caused by the inhomogeneous swelling of the PDMS stamp. Because the edges of the PDMS channel have more surface area exposed to toluene, the edges achieved a higher degree of swelling than the inner region. This inhomogeneous swelling of the PDMS in toluene caused the micelle solution to collect toward the centerline of the PDMS features, an effect that has been documented previously in the μCP of a poly(styrene-*alt*-maleic anhydride)/tetrahydrofuran system.[9] In the present case, once the toluene evaporated, the PS-*b*-PAA micellar thin film was kinetically trapped on the surfaces of the stamp features because the continuous PS matrix has a glass transition temperature that is well above room temperature.

Figure 2 shows the AFM characterization of a PS-*b*-PAA micellar thin film patterned by using a PDMS stamp with a channel width of 7 μm and a periodicity of 14 μm. Figure 2a shows an AFM height image of the substrate after stamping. The thickness of the patterned micellar thin films is demonstrated in Figure 2b, which shows an individual scan line between the two triangles shown in Figure 2a. This shows that the patterned stripes are approximately 100 nm thick and are uniform in shape. To confirm that the micellar substructure persisted in the patterned areas, we examined the areas indicated by the white squares in Figure 2a at higher resolution. Figure 2c shows the AFM phase image of the patterned micellar thin film that is located in the square labeled "c" in Figure 2a. The observed structure is identical to previous AFM images of micellar thin films[15,16] of this same block copolymer, and verifies the nanoscale substructure of the patterned thin films. Figure 2d shows the AFM phase image of the area indicated by the square labeled "d" in Figure 2a and corresponds to the smooth structure of the bare Si substrate. From these AFM results, we are able to conclude that our μCP procedure enables the creation of substrates with well-defined patterns of PS-*b*-PAA micellar thin films. The thickness of the patterned stripes suggests there are 4−5 layers of micelles, compared to the micellar monolayers created using a spin-casting approach.[14,16] The cracks observed in Figure 2a are believed to arise from stresses that are imparted to the glassy polymer thin films during the handling of the PDMS stamp during the stamping procedure. We have found that these cracks can be minimized by delicately handling the PDMS stamps during the stamping procedure.

Using this PS-*b*-PAA micellar system, we recently demonstrated the ability to create iron oxide nanocluster catalysts for the vertical growth of MWCNTs.[26] This was accomplished by varying the chemical vapor deposition growth parameters, the substrate, and the uniformity of the micellar thin film to discover a set of conditions that yielded dense growth of MWCNTs. In this report, we combine our knowledge of conditions for CNT synthesis using this catalyst system with the ability to pattern these catalysts using a μCP approach. The SEM micrographs in Figure 3 show the result for CNT growth using patterned stripes of iron oxide nanocluster arrays with widths of 1 μm and a periodicity of 10 μm (patterned using a channeled PDMS stamp with a width of 5 μm and a periodicity of 10 μm). The images show dense "walls" of MWCNTs that have grown vertically from the substrate. It is clear that these CNTs, which were grown from a patterned strip of catalyst nanoclusters, retain the individual shape of the underlying pattern, even though the height of these structures is roughly 2 orders of magnitude larger than the width of the patterns. Similar results have been observed for the vertical growth of CNTs using thin metal films patterned by electron beam evaporation.[22,23]

The SEM micrographs in Figure 4 show the result of CNT growth using an iron oxide nanocluster array patterned using a PDMS stamp of cylindrical posts with diameters of 4 μm and a periodicity of 8 μm using a removal velocity of 0.2 mm s^{-1} and an applied stress of 600 kPa. Reducing the removal velocity from 1 mm s^{-1} (Figure 1b) to 0.2 mm s^{-1} and increasing the applied stamping stress from 40 kPa (Figure 1b) to 600 kPa resulted in a transferred micellar thin film that, as shown in Figure 4a, was the negative of the original PDMS stamp. Figure 4b shows a representative result from the CNT growth, while Figure 4c shows the edge of the patterned area to demonstrate the vertical aspect of the growth. As in the CNT growth from channeled catalysts, it is clear from Figure 4 that the CNTs were catalyzed only from the patterned areas of the substrate. The CNTs also clearly maintain the patterned structure as they grow vertically from the substrate, even though the aspect ratio of the cylindrical columns is approximately 100. The MWCNT structures grown from the continuous circular pattern in Figure 4 appear to maintain the dimensions of the patterned catalyst more faithfully than the MWCNT structures grown from strips of the patterned catalyst in Figure 3. We are currently unsure of the explanation for this observation, and we plan to continue to investigate this topic in the future.

Conclusions

We have demonstrated a route for creating patterned iron oxide nanocluster arrays from PS-*b*-PAA micellar thin films using a μCP approach. The patterned nanoclusters catalyze vertical growth of CNTs selectively on the patterned regions of the substrate. We used optical microscopy and AFM to characterize the structure of our substrates as well as to verify that the patterned thin films maintain their micellar structure. Because the micellar thin films are capable of acting as both templates to create inorganic nanoclusters and nanoreactors, we believe that the ability to pattern these block copolymer micellar thin films can be exploited in a variety of applications. Thus, we are continuing our investigation of μCP-patterned PS-*b*-PAA micellar thin films in studies of CNT and zinc oxide nanowire synthesis, as well as in investigations of the templating of biologically active molecules for modifying cell attachment and function.

Acknowledgment. The Institute for Soldier Nanotechnologies (ISN) facilities and Center for Material Science and Engineering (CMSE) Shared Experimental Facilities were used extensively in this work, and the assistance of Libby Shaw is gratefully acknowledged. We also thank Piljin Yoo and Marianne Terrot for their assistance in creating the PDMS stamps. This work is supported primarily by the MIT ISN (Project 3.17, Contract DAAD19-02-D-0002) and, in part, by the National Science and Defense Engineering Graduate (NDSEG) Fellowship. A.J.H. is grateful for the support of a Fannie and John Hertz Foundation Fellowship, and the CNT synthesis facilities were maintained with support from NSF Grant DMI-0521985.

LA061054A